JOC The Journal of Organic Chemistry

Note

pubs.acs.org/joc

Fine-Tuning the Oxidative Ability of Persistent Radicals: Electrochemical and Computational Studies of Substituted 2-Pyridylhydroxylamines

Justin A. Bogart, Heui Beom Lee, Michael A. Boreen, Minsik Jun, and Eric J. Schelter*

P. Roy and Diana T. Vagelos Laboratories, Department of Chemistry, University of Pennsylvania, 231 South 34th Street, Philadelphia, Pennsylvania 19104, United States

Supporting Information

ABSTRACT: *N-tert*-Butyl-*N*-2-pyridylhydroxylamines were synthesized from 2-halopyridines and 2-methyl-2-nitrosopropane using magnesium−halogen exchange. The use of Turbo Grignard generated the metallo-2-pyridyl intermediate more reliably than alkyllithium reagents. The hydroxylamines were characterized using NMR, electrochemistry, and density functional theory. Substitution of the pyridyl ring in the 3-, 4-, and 5-positions was used to vary the potential of the nitroxyl/oxoammonium redox couple by 0.95 V. DFT computations of the electrochemical properties agree with experiment and provide a toolset for the predictive design of pyridyl nitroxides.

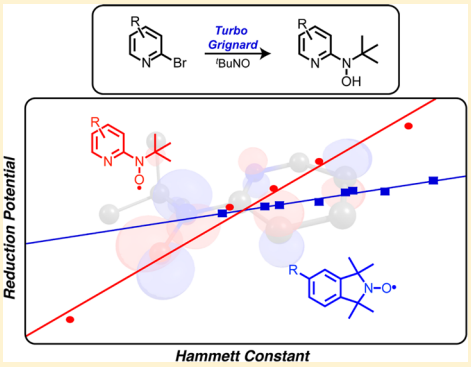

Nitroxides are an important class of compounds with diverse uses in catalytic, medicinal, and materials chemistry. Derivatives of the stable nitroxide radical, 2,2,6,6-tetramethylpiperidine-*N*-oxyl (TEMPO), have been used as oxidation catalysts for primary and secondary alcohols both in their free-radical form and complexed to metal ions such as Cu^{II}.[1−3] Recently, complexes of $FeCl_3$ and $AlCl_3$ were also shown to activate TEMPO toward oxidation chemistry.[4] In medicinal chemistry, open-shell nitroxides are used as spin probes[5] and have been shown to act as superoxide dismutase mimics.[6,7] They are being explored as potential therapeutic agents to control the concentration of deleterious reactive oxygen and nitrogen species.[8] Materials applications include the incorporation of nitroxides into dye-sensitized solar cells as redox mediators;[9,10] they have also been used as building blocks in the synthesis of molecular-based magnetic materials.[11−15] In all of these applications, the key characteristic of nitroxides is their stability in the open-shell form, which is typically modulated through substituents on an aliphatic backbone.[16−18]

We recently became interested in applying nitroxides in coordination chemistry as open-shell, redox-active ligands.[4,19,20] To explore a range of behavior in this context it is necessary to have access to nitroxides whose SOMO energies can be systematically varied through simple substitution.

Reported synthetic and theoretical studies of nitroxides highlight the ability to tune the redox potentials by derivatization of the nitroxide backbone through aliphatic substituents.[16,17,21] However, the reported studies typically focus on conservation of the structural motif of TEMPO where the π^*-type SOMO is localized on the N−O bond and substituent effects are confined to σ-inductive effects. For example, Bottle and co-workers synthesized a number of 4-substituted piperidine, isoindoline, and azaphenalene derivatives that each have the nitroxide moiety one sp^3 carbon atom removed from the conjugated π system.[17] In the case of the isoindoline nitroxides, a range of 0.16 V in the redox potentials of the nitroxyl/oxoammonium event was observed depending on substituents.

In contrast, there have been few studies that explore the redox properties of aromatic nitroxides, though Xu and co-workers have studied the substituent effects on redox potential for a series of *N*-(4-R-phenyl)hydroxamic acids.[18,22−24] To the best of our knowledge, there are no reports of nitroxides conjugated with aromatic systems that include electrochemical and theoretical studies. To accomplish our goal of an easily tuned system of nitroxides suitable for use as ligands in coordination chemistry, we sought to perform electrochemical and theoretical studies on *N-tert*-butyl-*N*-(2-pyridyl) nitroxides where the nitroxide is in direct conjugation with a heterocyclic ring system. Our hypothesis for this work was that the stability of the nitroxide could be tuned simply, and to a larger extent than reported aliphatic nitroxides by using electron-donating substituents in direct conjugation with the −(^{t}Bu)NO group.

Herein we report a novel and convenient synthesis of a series of *N-tert*-butyl-*N*-(2-R-pyridyl)hydroxylamines, R = 4-NMe_2 (**1**), 5-NMe_2 (**2**), 3-OMe (**3**), 5-SMe (**4**), 5-Me (**5**), H (**6**), and 5-CF_3 (**7**). These substitutions of the pyridine ring within the series adjust the nitroxide radical/oxoammonium redox

Received: May 2, 2013
Published: May 30, 2013

dx.doi.org/10.1021/jo400944r | J. Org. Chem. 2013, 78, 6344−6349

potential by 0.95 V. A semiempirical correlation between Hammett parameters and nitroxyl oxidation potentials is presented. Theoretical results show good agreement with the experimental solution electrochemical data, providing a toolset for predictive design of new pyridyl nitroxides.

The synthesis of compound **6** was reported previously (Scheme 1).[14] However, in our hands, attempts to cleanly

Scheme 1. Reported Synthesis of the Hydroxylamine 6 in 41% Yield

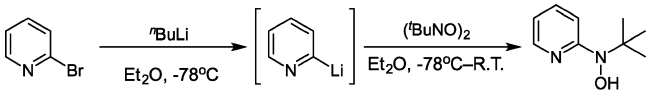

generate the 2-lithiopyridine using ^{n}BuLi at the reported temperature of −78 °C failed, invariably producing butylated addition products. Thus, we turned to the use of isopropylmagnesium chloride lithium chloride complex (Turbo Grignard) pioneered by Knochel and co-workers for the metal−halogen exchange reactions.[25−33] The reaction between the 2-halopyridines and Turbo Grignard generated the 2-pyridylmagnesium chloride species in situ affording clean conversion to hydroxylamines **1** and **3**−**7** upon addition of 2-methyl-2-nitrosopropane and quenching with degassed $NH_4Cl_{(aq)}$. Both electron-donating and -withdrawing substituents were tolerated using this protocol (Table 1), with one exception: the use of Turbo Grignard to produce hydroxylamine **2** with its 5-NMe_2 group led to incomplete conversion. In the case of **2**, ^{n}BuLi was required to synthesize the

Table 1. Synthesis of *N*-*tert*-Butyl-*N*-2-pyridylhydroxylamines

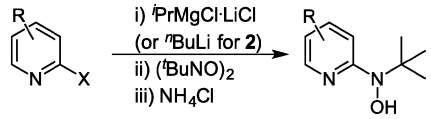

X = Br or I **1–7**

Entry	Precursor	Product	Time[a], h	Temp[a], °C	Yield[b], %
1		**1**	3 / 3	0→20 / 0	68
2	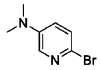	**2**	3/3	–100/–100→20	64
3		**3**	14 / 3	0→20 / 0	69
4		**4**	3/3	0→20 / 0	63
5		**5**	3 / 3	0→20 / 0	62
6		**6**	1 / 3	0→20 / 0	80
7		**7**	2 / 3	–78 / –78[c]	74

[a]Values are for reaction conditions during the first/second steps. [b]Isolated yields. [c]A complex mixture resulted if the reaction was not cooled to −78 °C.

compound in good yield (vide infra). The rate of the halogen exchange reaction was highly dependent on the pyrdine ring substituents, with electron-withdrawing substituents accelerating the reaction.

With the strongly donating 5-NMe_2 substituent on the pyridyl ring, the magnesium−halogen exchange reaction to generate the 2-pyridylmagnesium chloride species in situ only proceeded in 50% conversion. Therefore, in order to synthesize **2** in good yield, ^{n}BuLi was used instead. Addition of ^{n}BuLi at −100 °C cleanly afforded the 2-lithiopyridine species free of butylated addition products. The 2-lithiopyridine was then treated with 2-methyl-2-nitrosopropane at −100 °C and warmed to room temperature to produce compound **2** upon quenching. The hydroxylamines **1**−**7** were isolated either by recrystallization or by sublimation. These hydroxylamines were conveniently stored as solids under an N_2 atmosphere. Upon exposure to air, compounds **1**−**7** slowly oxidized to their free radical forms as indicated by their conversion to red oils.

With the compounds **1**−**7** in hand, we next turned to evaluation of their redox properties through solution electrochemistry. Figure 1 shows the cyclic voltammogram of

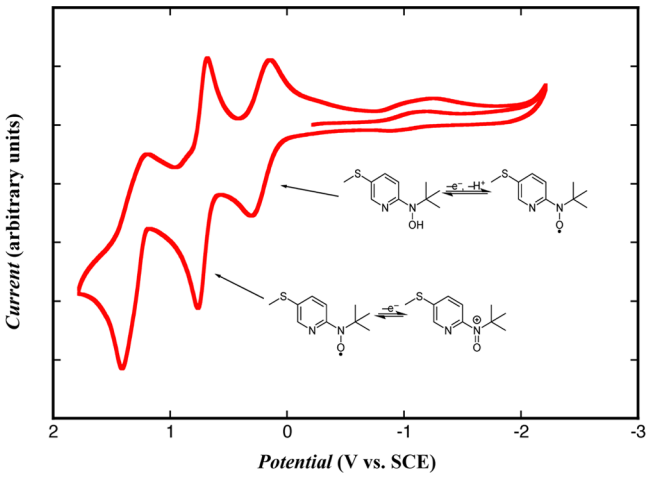

Figure 1. Cyclic voltammogram of the hydroxylamine **4** recorded in 0.1 M $[^nBu_4N][PF_6]$ CH_3CN.

hydroxylamine **4**, which is similar to the other derivatives. As observed for **1**−**7**, reported electrochemical data for nitroxides typically include two primary processes for the [N−O•]/[N−OH] and [N═O$^+$]/[N−O•] redox events. For the CV of **4** shown in Figure 1, the open circuit potential was measured at −0.24 V, indicating the wave at $E_{1/2}$ = 0.27 V was an oxidation. The oxidation was assigned to the [N−O•]/[N−OH] couple. In general, the behavior of the [N−O•]/[N−OH] couple is complicated by an associated proton transfer and is typically irreversible in acidic media. Indeed, we observed the first oxidation processes to the radical forms of **1**−**7** were poorly defined in the electrochemical experiments (see the Supporting Information). In all cases for **2**−**7**, the [N−O•]/[N−OH] couples were followed by second quasi-reversible oxidation waves at higher potentials, in the range $E_{1/2}$ = 0.24−1.17, which were assigned to [N═O$^+$]/[N−O•] redox events. Based on the complication of associate proton transfer for the [N−O•]/[N−OH] couples, our assessment of the relative energetics of **1**−**7** was made using the [N═O$^+$]/[N−O•] redox couple.

Table 2 shows the observed redox potentials for the [N═O$^+$]/[N−O•] couples for the hydroxylamines **1**−**7**. In general,

dx.doi.org/10.1021/jo400944r | J. Org. Chem. 2013, 78, 6344−6349

Table 2. Redox Potentials for the [N═O⁺]/[N−O•] Couple of Hydroxylamines 1−7 Referenced vs SCE

compd	E_{pa}	E_{pc}	$E_{1/2}$	ΔE	i_{pa}/i_{pc}
1	0.91				
2	0.29	0.19	0.24	0.10	1.08
3	0.79	0.72	0.76	0.07	1.36
4	0.83	0.73	0.78	0.10	1.07
5	0.90	0.84	0.87	0.06	1.52
6	1.05	0.95	1.00	0.10	2.02
7	1.23	1.10	1.17	0.13	2.55

the oxidation waves, E_{pa}, shift toward more negative values with increased electron-donating ability of the *ortho* or *para* substituent. In reported work by Rychnovsky et al.,[34] the ratio of i_{pa}/i_{pc} was used to assess the stability of the oxoammonium cation formed during the voltammetric scan, with values closer to unity indicating an increased stability of the oxoammonium species. Our results for **1**−**7** indicate that the oxoammonium species is stabilized by more donating substituents *ortho* or *para* to the ^{t}BuNO group.

Figure 2 shows a roughly linear relationship between the redox potentials for the [N═O⁺]/[N−O•] redox couple and

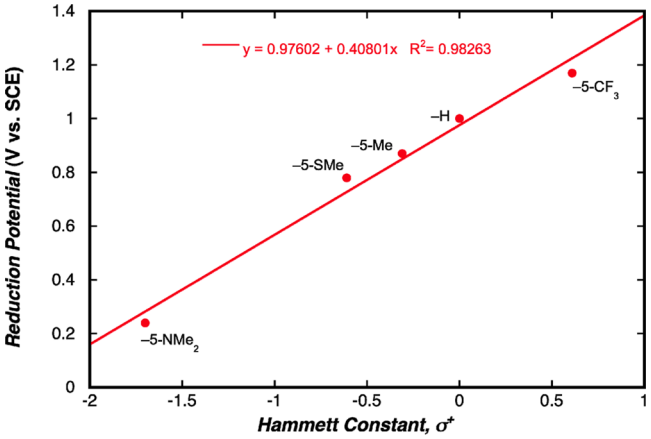

Figure 2. Hammett plot of the constants σ^+ for the *para*-substituents versus redox potential for the [N═O⁺]/[N−O•] couple of hydroxylamines **2** and **4**−**7**.

the Hammett constant σ^+ of the *para*-substituents for the series of 5-substituted compounds. A modest negative curvature is present in the Hammett plot despite the use of the σ^+ values. However, when the reduction potentials were plotted versus the inductive-only Hammett constant σ,[35] a pronounced negative curvature was evident and the linear relationship completely broke down, indicating there is significant bond resonance between the substituent in the 5-position and the ^{t}BuNO moiety. It is evident that the σ^+ values provide the most useful linear free energy model for the pyridyl nitroxide system.[35]

The slope of 0.41 provided by the linear fit of these data provides a metric for the sensitivity of the nitroxide redox potential to pyridyl substitution (Figure 2). An analogous relationship between oxoammonium/radical nitroxide potentials and substituents can be developed for TEMPO-derived, aliphatic nitroxide radicals using the simple Hammett constants, σ.[17] In the case of the reported isoindolines a slope of 0.11 is found (see the Supporting Information), indicating that the redox potentials of the pyridyl nitroxides are ∼4 times more sensitive to substituent effects of the pyridyl ring system than in the isoindoline cases.[17] Using the same metric, the pyridyl nitroxide system studied in this work is ∼2 times more sensitive to substituent effects than the *N*-phenylhydroxamic acid system.[36]

In order to develop a toolset for the predictive design of new pyridyl nitroxides, we performed DFT calculations on the nitroxyl radical analogues of compounds **1**−**7**. Methods for estimating the half-wave oxidation potentials of nitroxyl radicals have been developed for those bearing aliphatic structural frameworks.[16] The redox potentials of aliphatic nitroxides have been predicted with a high degree of accuracy,[17] and these predictions are improved through the use of a solvent continuum in the calculation.[34] In the current work, we applied a B3LYP hybrid DFT method. Geometry optimizations were carried out using the 6-31G* basis set and the CPCM SCRF method with acetonitrile as the solvent. The default UFF radius was used.

The geometries of the nitroxyl radical of compounds **1**−**7** and their oxoammonium forms were optimized using DFT methods that included effects for acetonitrile solvation (see the Supporting Information for details).[37−39] Changes in the free energies for reactions $\Delta G_{rxn} = \Sigma(G_{product}) - \Sigma(G_{reactant})$ were obtained using the zero-point energy corrected free energy values obtained from frequency calculations. The SOMOs for the radical forms of **1**−**7** show delocalization into the aromatic ring, especially onto the 1-, 3-, and 5-positions (see the Supporting Information). Substituents at the 3- and 5-positions were therefore expected to affect the energy of the SOMO, as observed in the electrochemical results.

Following the method reported by Gillmore and co-workers for diverse organic compounds,[40] the calculated free energy difference between the oxidized and neutral forms were correlated with the observed electrochemical oxidation potentials. Calculated ΔG values (Table S1, Supporting Information) are plotted against the observed oxidation potentials in Figure 3. Remarkably good correlation is found

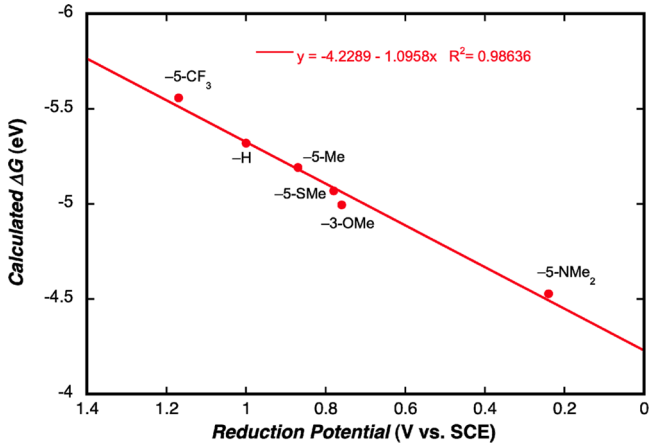

Figure 3. Observed potential vs the difference in free energy between the *N*-oxoammonium cation and the nitroxide radical.

between the calculated and observed results. For the predicted half-wave potentials, a mean absolute deviation of 30 mV from the experimentally determined values was obtained,[21] supporting the validity of the applied computational model for the pyridyl nitroxides. Compound **1** was not included in the correlation because the observed oxidation is irreversible and

dx.doi.org/10.1021/jo400944r | J. Org. Chem. 2013, 78, 6344−6349

$E_{1/2}$ could not be accurately determined. Nevertheless, the calculated ΔG value for this compound is similar to that for compound **5**, in agreement with their similar σ^+ Hammett parameters and the similarity in anodic peak potentials between the two compounds. The semiempirical correlations established by the data shown in Figures 2 and 3 establish a useful groundwork for the prediction of the pyridyl-based nitroxyl oxidation potentials based upon calculated values of ΔG.

We have demonstrated reliable syntheses for a series of pyridyl-appended hydroxylamines using metal−halogen exchange reactions. Compounds **1** and **3**−**7** were prepared using solutions of Turbo Grignard to accomplish metal−halogen exchange instead of solutions of ^{n}BuLi. However, for the highly donating $-NMe_2$ substituent in the 5-position of the pyridine ring, ^{n}BuLi was required to accomplish the synthesis of the pyridyl hydroxylamine in high yield. The substituent effects within this system give a 4-fold greater sensitivity to tuning the oxoammonium/radical nitroxide redox potential compared to aliphatic nitroxides, such as TEMPO variants. DFT calculations reproduce this sensitivity of the nitroxide oxidation potential to substiutents, providing a predictive toolset for the design of new aryl nitroxides in silico.

EXPERIMENTAL SECTION

Reaction of 2-Halopyridines with 2-Methyl-2-nitrosopropane Dimer. General Procedure.

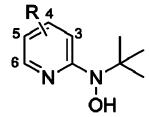

An N_2-purged Schlenk flask equipped with a magnetic stirrer was charged with halopyridine (1 equiv) and cooled to 0 °C. A 1.3 M solution of isopropylmagnesium chloride lithium chloride complex in THF (1.1−2 equiv) was added, and the reaction was allowed to slowly warm to room temperature where it was reacted for 3 h. The solution was cooled to 0 °C, and a clear blue THF solution of 2-methyl-2-nitrosopropane dimer (1 equiv) was added. After reacting for another 3 h, the reaction was quenched with a degassed saturated aqueous NH_4Cl solution. The organic layer was extracted under an N_2 atmosphere with Et_2O by syringing the Et_2O layer into a separate N_2 purged Schlenk flask. The organic extracts were dried over $MgSO_4$, and the organic layer was isolated by cannula filtration into another N_2-purged Schlenk flask. Volatiles were removed under reduced pressure and *N*-*tert*-butyl-*N*-2-pyridylhydroxylamine was isolated by sublimation or recrystallization in 60−80% yield.

***N*-*tert*-Butyl-*N*-2-[4-(dimethylamino)pyridyl]hydroxylamine (1).** A 50 mL Schlenk flask was charged with a solution of 2-iodo-4-(dimethylamino)pyridine (1.00 g, 4.03 mmol, 1 equiv) in THF (5 mL). A 1.3 M solution of isopropylmagnesium chloride lithium chloride complex in THF (3.8 mL, 4.94 mmol, 1.23 equiv) was added dropwise at 0 °C, and the mixture was slowly warmed to room temperature. The mixture was stirred at room temperature for 3 h. A separate Schlenk flask was charged with a solution of 2-methyl-2-nitrosopropane dimer (0.77 g, 4.4 mmol, 1.1 equiv) in THF (10 mL). The resulting blue solution was added to the reaction flask by cannula transfer at 0 °C, and the mixture was stirred for 3 h. A saturated, degassed, aqueous solution of ammonium chloride (∼25 mL) was added to quench the reaction. The aqueous layer was extracted with degassed CH_2Cl_2, and the organic extracts were syringed into an N_2-purged Schlenk flask. The extracts were dried over $MgSO_4$ and filtered by cannula transfer into an N_2-purged Schlenk flask. The filtrate was concentrated under reduced pressure to yield a crude tan solid. Compound **1** was isolated as colorless crystals by layering hexane onto a saturated DME solution at −35 °C. The crystals were isolated by filtration and dried under reduced pressure: yield 0.57 g, 68%; mp 115 °C dec; ^{1}H NMR (500 MHz, C_6D_6) δ 8.49 (s, 1H), 8.01 (d, J = 5.9 Hz, 1H), 6.35 (d, J = 2.4 Hz, 1H), 5.87 (dd, J = 5.9, 2.4 Hz, 1H), 2.27 (s, 6H), 1.42 (s, 9H); ^{13}C NMR (125.8 MHz, C_6D_6) δ 163.9, 155.7, 146.9, 104.3, 100.1, 61.8, 38.9, 27.5; FT-IR (KBr, cm^{-1}) 3295, 2984, 1598, 1531, 1512, 1449, 1369, 1224, 1158, 1006, 962, 843, 809, 631; HRMS (ESI) m/z calcd for $C_{11}H_{20}N_3O$ (M + H) 210.1606, found 210.1605.

Synthesis of *N*-*tert*-Butyl-*N*-2-[5-(dimethylamino)pyridyl]-hydroxylamine (2). A 50 mL Schlenk flask was charged with a solution of 2-bromo-5-(dimethylamino)pyridine (0.33 g, 1.6 mmol, 1 equiv) in Et_2O (10 mL) and cooled to −100 °C in an Et_2O/dry ice bath. To this colorless slurry was added dropwise a solution of ^{n}BuLi in hexanes (1.0 mL, 1.6 mmol, 1 equiv). The resulting yellow slurry was allowed to stir for 3 h. 2-Methyl-2-nitrosopropane (0.285 g, 1.6 mmol, 1 equiv) dissolved in Et_2O was added dropwise, and the reaction turned orange. This mixture was slowly brought to room temperature and stirred for 3 h producing a green solution. The reaction was quenched with a degassed, saturated aqueous solution of ammonium chloride, producing a red solution. The aqueous layer was extracted with degassed Et_2O, and the organic extracts were syringed into an N_2 purged Schlenk flask. The extracts were dried over $MgSO_4$ and filtered by cannula transfer into an N_2-purged Schlenk flask. The filtrate was concentrated under reduced pressure to yield a crude tan solid. Compound **1** was isolated as colorless crystals by layering hexane onto a saturated DME solution at −35 °C. The crystals were isolated by filtration and dried under reduced pressure: yield 0.21 g, 64%; mp 103 °C dec; ^{1}H NMR (500 MHz, C_6D_6) δ 8.00 (s, 1H), 7.79 (d, J = 3.2 Hz, 1H), 7.04 (d, J = 8.9 Hz, 1H), 6.55 (dd, J = 8.9, 3.2 Hz, 1H), 2.32 (s, 6H), 1.34 (s, 9H); ^{13}C NMR (125.8 MHz, C_6D_6) δ 153.3, 144.4, 131.7, 121.4, 119.0, 61.6, 40.3, 27.0; FT-IR (KBr, cm^{-1}) 3196, 2974, 1593, 1555, 1497, 1446, 1388, 1360, 1272, 1215, 1125, 1062, 1010, 944, 875, 829, 809, 756, 682, 638, 538; HRMS (ESI) m/z calcd for $C_{11}H_{20}N_3O$ (M + H) 210.1606, found 210.1605.

Synthesis of *N*-*tert*-Butyl-*N*-2-(3-methoxypyridyl)-hydroxylamine (3). A 250 mL Schlenk flask was charged with a solution of 2-iodo-3-methoxypyridine (2.02 g, 8.6 mmol, 1 equiv) in THF (20 mL). A 1.3 M solution of isopropylmagnesium chloride lithium chloride complex in THF (7.3 mL, 9.5 mmol, 1.1 equiv) was added dropwise at 0 °C, and the mixture was allowed to slowly warm to room temperature over 12 h. A separate Schlenk flask was charged with a solution of 2-methyl-2-nitrosopropane dimer (1.00 g, 5.7 mmol, 0.67 equiv) in THF (10 mL). The resulting blue solution was added to the reaction flask via cannula at 0 °C and slowly warmed to room temperature. Stirring was continued for 3 h at room temperature. A saturated, degassed, aqueous solution of ammonium chloride (5 mL) was added to quench the reaction. The volatiles were removed under reduced pressure, and the organic product was extracted with THF. The filtrate was concentrated under reduced pressure to yield a creamy yellow solid. This solid was suspended in toluene and stirred with gentle heating until dissolved. This saturated solution was then cooled to −35 °C, resulting in the precipitation of compound **3** as a white powder. The solid was isolated by filtration over a medium porosity fritted filte: yield 1.16 g, 69%; mp 130 °C dec; ^{1}H NMR (500 MHz, C_6D_6): δ 7.84 (dd, J = 4.5, 1.5 Hz, 1H), 7.21 (s, 1H), 6.49 (dd, J = 8.0, 4.5 Hz, 1H), 6.41 (dd, J = 8.0, 1.5 Hz, 1H), 3.10 (s, 3H), 1.45 (s, 9H); ^{13}C NMR (125.8 MHz, C_6D_6): δ 153.7, 150.4, 138.5, 121.2, 119.6, 62.2, 55.4, 26.5; FT-IR (KBr, cm^{-1}) 3611, 2977, 1591, 1577, 1465, 1430, 1370, 1283, 1227, 1193, 1126, 1018, 806; HRMS (ESI) m/z calcd for $C_{10}H_{16}N_2O_2$ (M + H) 197.1290, found 197.1291.

Synthesis of *N*-*tert*-Butyl-*N*-2-[5-(methylthio)pyridyl]-hydroxylamine (4). 2-Bromo-5-(methylthio)pyridine (0.58 g, 2.8 mmol, 1 equiv) dissolved in THF (5 mL) was added to an N_2-purged Schlenk flask and cooled to 0 °C. A 1.3 M solution of isopropylmagnesium chloride lithium chloride complex in THF (4.3 mL, 5.6 mmol, 2 equiv) was added dropwise at this temperature. The flask was removed from the ice bath and allowed to slowly warm to room temperature where it was reacted for 3 h. The flask was then cooled to 0 °C, and a THF solution (5 mL) of 2-methyl-2-nitrosopropane dimer (0.74 g, 4.2 mmol, 1.5 equiv) was added. After 3 h, the reaction was quenched with degassed aqueous NH_4Cl. The aqueous layer was extracted with 3 × 20 mL of Et_2O under an N_2

dx.doi.org/10.1021/jo400944r | J. Org. Chem. 2013, 78, 6344−6349

atmosphere. The organic extracts were dried with $MgSO_4$, which was filtered off by cannula filtration, and the solvent was removed under reduced pressure, yielding a crude tan solid. Layering of pentane onto an Et_2O solution of this crude solid lead to the deposition of colorless crystals of **4** which were collected by filtration: yield 0.37 g, 63%; mp 61.8−62.9 °C; ^{1}H NMR (500 MHz, C_6D_6) δ 8.18 (dd, J = 2.5, 0.9 Hz, 1H), 7.33 (s, 1H), 7.11 (dd, J = 8.6, 2.5 Hz, 1H), 6.93 (dd, J = 8.6, 0.9 Hz, 1H), 1.86 (s, 3H), 1.29 (s, 9H); ^{13}C NMR (125.8 MHz, C_6D_6) δ 161.2, 146.3, 137.5, 129.4, 117.1, 62.3, 27.3, 17.1; FT-IR (KBr, cm^{-1}) 3086, 3929, 1571, 1553, 1477, 1432, 1393, 1366, 1260, 1199, 1108, 1013, 964, 950, 921, 846, 834, 741, 665, 626, 549, 473; HRMS (ESI) m/z calcd for $C_{10}H_{17}N_2OS$ (M + H) 213.1062, found 213.1069.

Synthesis of *N*-*tert*-Butyl-*N*-2-(5-methylpyridyl)-hydroxylamine (5). Compound **5** was synthesized from the action of 2-bromo-5-methylpyridine (1.0 g, 5.8 mmol, 1 equiv) with a 1.3 M THF solution of isopropylmagnesium chloride lithium chloride complex in THF (5.4 mL, 7.0 mmol, 1.2 equiv) at 0 °C. The solution was allowed to warm to room temperature and react for 3 h. The reaction was placed back into the 0 °C ice bath, and a THF solution (10 mL) of 2-methyl-2-nitrosopropane dimer was then added (1.01 g, 5.8 mmol, 1 equiv). The reaction was quenched after an additional 3 h with a saturated aqueous ammonium chloride solution that had been sparged with N_2 prior to addition. The organic layer was removed, and the aqueous layer was extracted under an N_2 atmosphere with 3 × 15 mL of Et_2O. The combined organic extracts were dried with $MgSO_4$, and the organic layer was isolated by cannula filtration. Solvents were removed in vacuo, and the crude tan solid was sublimed at 50 °C and 0.1 Torr: yield 0.65 g, 62%; mp 64.1−65.5 °C; ^{1}H NMR (500 MHz, C_6D_6) δ 7.97 (s, 1H), 7.75 (s, 1H), 6.92 (d, J = 8.2 Hz, 1H), 6.84 (d, J = 8.2 Hz, 1H), 1.77 (s, 3H), 1.31 (s, 9H); ^{13}C NMR (125.8 MHz, C_6D_6) δ 160.9, 146.9, 137.7, 117.3, 62.0, 27.2, 17.7; FT-IR (KBr, cm^{-1}) 3190, 2990, 1597, 1474, 1359, 1210, 1026, 957, 855, 675; HRMS (ESI) m/z calcd for $C_{10}H_{17}N_2O$ (M + H) 181.1341, found 181.1336.

Synthesis of *N*-*tert*-Butyl-*N*-(2-pyridyl)hydroxylamine (6). Compound **6** was synthesized by modification of a previously reported procedure.[14] A 50 mL Schlenk flask was charged with 2-bromopyridine (0.8 mL, 8.4 mmol, 1 equiv). A 1.3 M solution of isopropylmagnesium chloride lithium chloride complex in THF (8.8 mL, 11.4 mmol, 1.35 equiv) was added dropwise at 0 °C, and the reaction was allowed to warm to room temperature. The solution was stirred at rt for 1 h. A separate Schlenk flask was charged with a solution of 2-methyl-2-nitrosopropane dimer (0.89 g, 5.1 mmol, 0.6 equiv) in THF (10 mL). The resulting blue solution was added to the reaction flask via cannula at 0 °C and stirred for 3 h. A saturated, degassed, aqueous solution of ammonium chloride (5 mL) was added under N_2 to quench the reaction. The organic layer was removed, and the aqueous layer was extracted under an N_2 atmosphere with 3 × 15 mL of Et_2O. The combined organic extracts were dried with $MgSO_4$, and the organic layer was isolated by cannula filtration. The organic layer was concentrated under reduced pressure to yield a crude tan solid. Compound **6** was isolated as colorless crystals after sublimation at 35 °C and 0.2 Torr: yield 1.12 g, 80%; mp 44.7−45.4 °C (lit.[14] 40−42 °C); ^{1}H NMR (500 MHz, C_6D_6) δ 8.08 (ddd, J = 4.9, 2.0, 0.5 Hz, 1H), 7.66 (s, 1H), 6.99 (ddd, J = 8.6, 6.6, 2.0 Hz, 1H) 6.97 (ddd, J = 8.6, 1.5, 0.5 Hz, 1H), 6.40 (ddd, J = 6.6, 4.9, 1.5 Hz, 1H), 1.30 (s, 9H); ^{13}C NMR (125.8 MHz, C_6D_6) δ 163.6, 147.0, 137.1, 118.9, 117.2, 62.2, 27.3; FT-IR (KBr, cm^{-1}) 2972, 1597, 1465, 1429, 1360, 1273, 1200, 1027, 932, 748, 702; HRMS (ESI) m/z calcd for $C_9H_{15}N_2O$ (M + H) 167.1184, found 167.1183.

Synthesis of *N*-*tert*-Butyl-*N*-2-[5-(trifluoromethyl)pyridyl] hydroxylamine (7). A 50 mL Schlenk flask was charged with a solution of 2-iodo-5-(trifluoromethyl)pyridine (0.29 g, 1.07 mmol, 1 equiv) in THF (∼5 mL). A 1.3 M solution of isopropylmagnesium chloride−lithium chloride complex in THF (1.2 mL, 1.56 mmol, 1.45 equiv) was added dropwise at −78 °C and stirred for 2 h. A separate Schlenk flask was charged with a solution of 2-methyl-2-nitrosopropane dimer (0.35 g, 2 mmol, 2 equiv) in THF (5 mL). The resulting blue solution was added to the reaction flask via cannula at −78 °C and reacted for 3 h. A saturated, degassed, aqueous solution of ammonium chloride (5 mL) was added to quench the reaction. All volatiles were removed under reduced pressure, and the organic product was extracted with Et_2O. The filtrate was concentrated under reduced pressure to yield a creamy yellow solid. Compound **7** was isolated as a white solid after sublimation at 50 °C and 0.2 Torr: yield 0.19 g, 74%; mp 78.8−79.7 °C; ^{1}H NMR (500 MHz, C_6D_6) δ 8.33 (dd, J = 2.5, 1.0 Hz, 1H), 7.22 (dd, J = 8.8, 2.5 Hz, 1H), 6.74 (dd, J = 8.8, 1.0 Hz), 6.02 (s, 1H), 1.30 (s, 9H); ^{13}C NMR (125.8 MHz, C_6D_6) δ 165.4, 144.5 (q, J = 4.3 Hz), 134.3 (q, J = 3.3 Hz), 125.2 (q, J = 271.2 Hz), 119.9 (q, J = 32.9 Hz), 113.8, 63.0, 27.6; ^{19}F NMR (282.2 MHz, C_6D_6) δ −61.2 ppm; FT-IR (KBr, cm^{-1}) 3233, 2984, 1607, 1575, 1484, 1392, 1338, 1162, 1080, 854; HRMS (ESI) m/z calcd for $C_{10}H_{14}F_3N_2O$ (M + H) 235.1058, found 235.1059.

■ ASSOCIATED CONTENT

Ⓢ Supporting Information

Experimental details, NMR spectra, full electrochemical data, and DFT-optimized coordinates in the neutral and cationic forms for compounds **1**−**7**. This material is available free of charge via the Internet at http://pubs.acs.org.

■ AUTHOR INFORMATION

Corresponding Author

*E-mail: schelter@sas.upenn.edu.

Notes

The authors declare no competing financial interest.

■ ACKNOWLEDGMENTS

We gratefully acknowledge the Chemical Sciences, Geosciences, and Biosciences Division, Office of Basic Energy Sciences, Early Career Research Program of the U.S. Department of Energy, under Award Nos. DE-SC0006518 and DE-FG02-11ER16239 for support of this work. The University of Pennsylvania is also acknowledged for financial support. We thank the U.S. National Science Foundation for support of the computing cluster (CHE-0131132) used in this work. This work also used the Extreme Science and Engineering Discovery Environment (XSEDE), which is supported by U.S. National Science Foundation Grant No. OCI-1053575. J.A.B. thanks the NSF-GRF program for supporting his access to the XSEDE computing resource. We thank Dr. Nicholas A. Piro for assistance in preparing the TOC graphic.

■ REFERENCES

(1) De Luca, L.; Giacomelli, G.; Porcheddu, A. *Org. Lett.* **2001**, *3*, 3041−3043.
(2) Gamez, P.; Arends, I. W. C. E.; Reedijk, J.; Sheldon, R. A. *Chem. Commun.* **2003**, 2414−2415.
(3) Fey, T.; Fischer, H.; Bachmann, S.; Albert, K.; Bolm, C. *J. Org. Chem.* **2001**, *66*, 8154−8159.
(4) Scepaniak, J. J.; Wright, A. M.; Lewis, R. A.; Wu, G.; Hayton, T. W. *J. Am. Chem. Soc.* **2012**, *134*, 19350−19353.
(5) Nguyen, P.; Qin, P. Z. *Wiley Interdiscip. Rev. RNA* **2012**, *3*, 62−72.
(6) Goldstein, S.; Merenyi, G.; Russo, A.; Samuni, A. *J. Am. Chem. Soc.* **2002**, *125*, 789−795.
(7) Soule, B. P.; Hyodo, F.; Matsumoto, K.-i.; Simone, N. L.; Cook, J. A.; Krishna, M. C.; Mitchell, J. B. *Free Radical Bio. Med.* **2007**, *42*, 1632−1650.
(8) Hoye, A. T.; Davoren, J. E.; Wipf, P.; Fink, M. P.; Kagan, V. E. *Acc. Chem. Res.* **2008**, *41*, 87−97.
(9) Kato, F.; Kikuchi, A.; Okuyama, T.; Oyaizu, K.; Nishide, H. *Angew. Chem., Int. Ed.* **2012**, *51*, 10177−10180.
(10) Kato, F.; Hayashi, N.; Murakami, T.; Okumura, C.; Oyaizu, K.; Nishide, H. *Chem. Lett.* **2010**, *39*, 464−465.

(11) Likhtenshtein, G.; Yamauchi, J.; Nakatsuji, S.; Smirnov, A. I.; Tamura, R. In *Nitroxides: Applications in Chemistry, Biomedicine, and Materials Science*; Wiley-VCH: Weinheim, 2008.
(12) Okazawa, A.; Nagaichi, Y.; Nogami, T.; Ishida, T. *Inorg. Chem.* **2008**, *47*, 8859−8868.
(13) Osanai, K.; Okazawa, A.; Nogami, T.; Ishida, T. *J. Am. Chem. Soc.* **2006**, *128*, 14008−14009.
(14) Okazawa, A.; Nogami, T.; Ishida, T. *Chem. Mater.* **2007**, *19*, 2733−2735.
(15) Kanegawa, S.; Karasawa, S.; Maeyama, M.; Nakano, M.; Koga, N. *J. Am. Chem. Soc.* **2008**, *130*, 3079−3094.
(16) Gryn'ova, G.; Barakat, J. M.; Blinco, J. P.; Bottle, S. E.; Coote, M. L. *Chem.—Eur. J.* **2012**, *18*, 7582−7593.
(17) Blinco, J. P.; Hodgson, J. L.; Morrow, B. J.; Walker, J. R.; Will, G. D.; Coote, M. L.; Bottle, S. E. *J. Org. Chem.* **2008**, *73*, 6763−6771.
(18) Marx, L.; Schollhorn, B. *New J. Chem.* **2006**, *30*, 430−434.
(19) Evans, W. J.; Perotti, J. M.; Doedens, R. J.; Ziller, J. W. *Chem. Commun.* **2001**, 2326−2327.
(20) Lemaire, M. T. *Pure Appl. Chem.* **2004**, *76*, 277−293.
(21) Hodgson, J. L.; Namazian, M.; Bottle, S. E.; Coote, M. L. *J. Phys. Chem. A* **2007**, *111*, 13595−13605.
(22) Ziessel, R.; Ulrich, G.; C. Lawson, R.; Echegoyen, L. *J. Mater. Chem.* **1999**, *9*, 1435−1448.
(23) Suga, T.; Pu, Y.-J.; Oyaizu, K.; Nishide, H. *Bull. Chem. Soc. Jpn.* **2004**, *77*, 2203−2204.
(24) Xu, F.; Deussen, H.-J. W.; Lopez, B.; Lam, L.; Li, K. *Eur. J. Biochem.* **2001**, *268*, 4169−4176.
(25) Liu, C.-Y.; Ren, H.; Knochel, P. *Org. Lett.* **2006**, *8*, 617−619.
(26) Stoll, A. H.; Krasovskiy, A.; Knochel, P. *Angew. Chem., Int. Ed.* **2006**, *45*, 606−609.
(27) Kopp, F.; Wunderlich, S.; Knochel, P. *Chem. Commun.* **2007**, 2075−2077.
(28) Lin, W.; Chen, L.; Knochel, P. *Tetrahedron* **2007**, *63*, 2787−2797.
(29) Despotopoulou, C.; Bauer, R. C.; Krasovskiy, A.; Mayer, P.; Stryker, J. M.; Knochel, P. *Chem.—Eur. J.* **2008**, *14*, 2499−2506.
(30) Liu, C.-Y.; Knochel, P. *Org. Lett.* **2005**, *7*, 2543−2546.
(31) Ren, H.; Knochel, P. *Chem. Commun.* **2006**, 726−728.
(32) Ren, H.; Krasovskiy, A.; Knochel, P. *Chem. Commun.* **2005**, 543−545.
(33) Krasovskiy, A.; Knochel, P. *Angew. Chem., Int. Ed.* **2004**, *43*, 3333−3336.
(34) Rychnovsky, S. D.; Vaidyanathan, R.; Beauchamp, T.; Lin, R.; Farmer, P. J. *J. Org. Chem.* **1999**, *64*, 6745−6749.
(35) Hansch, C.; Leo, A.; Taft, R. W. *Chem. Rev.* **1991**, *91*, 165−195.
(36) Xu and co-workers report a slope of 0.14 for the correlation of anodic peak potentials for the second oxidation to substituent sigma minus values. Replotting these potentials versus the set of σ^+ values used in this work, however, we obtain a slope of 0.22.
(37) Gaussian 09, Revision A.02: Frisch, M. J.; Trucks, G. W.; Schlegel, H. B.; Scuseria, G. E.; Robb, M. A.; Cheeseman, J. R.; Scalmani, G.; Barone, V.; Mennucci, B.; Petersson, G. A.; Nakatsuji, H.; Caricato, M.; Li, X.; Hratchian, H. P.; Izmaylov, A. F.; Bloino, J.; Zheng, G.; Sonnenberg, J. L.; Hada, M.; Ehara, M.; Toyota, K.; Fukuda, R.; Hasegawa, J.; Ishida, M.; Nakajima, T.; Honda, Y.; Kitao, O.; Nakai, H.; Vreven, T.; Montgomery, J. A., Jr.; Peralta, J. E.; Ogliaro, F.; Bearpark, M.; Heyd, J. J.; Brothers, E.; Kudin, K. N.; Staroverov, V. N.; Kobayashi, R.; Normand, J.; Raghavachari, K.; Rendell, A.; Burant, J. C.; Iyengar, S. S.; Tomasi, J.; Cossi, M.; Rega, N.; Millam, N. J.; Klene, M.; Knox, J. E.; Cross, J. B.; Bakken, V.; Adamo, C.; Jaramillo, J.; Gomperts, R.; Stratmann, R. E.; Yazyev, O.; Austin, A. J.; Cammi, R.; Pomelli, C.; Ochterski, J. W.; Martin, R. L.; Morokuma, K.; Zakrzewski, V. G.; Voth, G. A.; Salvador, P.; Dannenberg, J. J.; Dapprich, S.; Daniels, A. D.; Farkas, O □.; Foresman, J. B.; Ortiz, J. V.; Cioslowski, J.; Fox, D. J. Gaussian, Inc., Wallingford, CT, 2009.
(38) Barone, V.; Cossi, M. *J. Phys. Chem. A* **1998**, *102*, 1995−2001.
(39) Cossi, M.; Rega, N.; Scalmani, G.; Barone, V. *J. Comput. Chem.* **2003**, *24*, 669−681.
(40) Lynch, E. J.; Speelman, A. L.; Curry, B. A.; Murillo, C. S.; Gillmore, J. G. *J. Org. Chem.* **2012**, *77*, 6423−6430.